New Journal of Physics
The open-access journal for physics

# Spiral wave drift and complex-oscillatory spiral waves caused by heterogeneities in two-dimensional *in vitro* cardiac tissues

**Sung-Jae Woo, Jin Hee Hong, Tae Yun Kim, Byung Wook Bae and Kyoung J Lee**[1]

CRI Center for Neurodynamics and Department of Physics, Korea University, Seoul 136-713, Korea
E-mail: kyoung@nld.korea.ac.kr

*New Journal of Physics* **10** (2008) 015005 (18pp)
Received 20 August 2007
Published 31 January 2008
Online at http://www.njp.org/
doi:10.1088/1367-2630/10/1/015005

**Abstract.** Understanding spiral reentry wave dynamics in cardiac systems is important since it underlies various cardiac arrhythmia including cardiac fibrillation. Primary cultures of dissociated cardiac cells have been a convenient and useful system for studying cardiac wave dynamics, since one can carry out systematic and quantitative studies with them under well-controlled environments. One key drawback of the dissociated cell culture is that, inevitably, some spatial inhomogeneities in terms of cell types and density, and/or the degree of gap junction connectivity, are introduced to the system during the preparation. These unintentional spatial inhomogeneities can cause some non-trivial wave dynamics, for example, the entrainment dynamics among different spiral waves and the generation of complex-oscillatory spiral waves. The aim of this paper is to quantify these general phenomena in an *in vitro* cardiac system and provide explanations for them with a simple physiological model having some realistic spatial inhomogeneities incorporated.

[1] Author to whom any correspondence should be addressed.

## Contents



## 1. Introduction

Spiral waves are observed in various nonequilibrium systems that have a two-dimensional (2D) spatial extension. Various examples are known to exist in a number of different biological as well as chemical systems. Some of the most well known examples in nonlinear chemistry are the Belousov–Zhabotinsky reaction–diffusion system [1]–[3], the chloride–iodide–malonic acid reaction–diffusion system [4, 5], the ferrocyanide–iodate–sulfite reaction–diffusion system [6]–[8], and catalytic oxidation of CO on Pt [9, 10]. There also exist many different examples in biology, and they have important biological and/or medical implications. Some well known examples are cyclic adenosine monophoshpate (cAMP) waves in populations of *Dictyostelium discoidium* cells [11]–[13], cardiac wave reentries [14]–[17], and calcium waves in oocytes [18, 19] and glia cell networks [20]. In all cases, the spiral wave activity either underlies an important biological function or has a physiological significance. For example, the emergence of calcium waves following fertilization and the subsequent, prolonged, elevation of calcium levels in the cytosol of oocytes is known to down-regulate the cell division [21].

The most important example of spiral waves is perhaps cardiac reentries from the viewpoint of medical applications. Spatiotemporal wave activities in heart tissue have long been a subject of numerous studies because they are responsible for cardiac arrythmia [14]–[17], [22]–[26]. Particular attention has been paid to the formation of spiral waves in the ventricles because there exists a substantial amount of evidence that it is the most prevailing cause for ventricular tachycardia which subsequently destabilizes into a ventricle fibrillation [15]–[17], [24, 26].

Investigating their properties are, however, expensive, and demanding tasks for a number of reasons, in particular, for large animal experiments. Firstly, the anatomical complexity of the intact heart often prevents one from making any easy interpretation of the observed cardiac waves and their instability. Secondly, it is practically difficult to keep the whole heart system under investigation viable and controlled for more than a day. Thirdly, the current imaging techniques for visualizing cardiac waves of the whole heart mostly rely on extrinsically introduced fluorescent dyes which are invasive to the system. More importantly, the fluorescent dyes bleach out in a few hours—a critical hindrance that makes a long-term experimental

investigation impossible. Multi-electrodes mapping is an alternative method that is free from the dye toxicity and bleaching effects, but in practice its spatial resolution is limited.

With all these drawbacks of *in vivo* heart studies, primary cultures of dissociated cardiac cells have been developed and used as a useful alternative to whole heart preparation [27]–[33]. Given the advancement in primary cell culture techniques over the years, one can now easily prepare several large cardiac culture dishes at a time and keep their viability for a long period of time (∼weeks) without much effort. Indeed, *in vitro* cardiac tissues have become a very useful subject for quantitative, parametric, studies of cardiac waves. One can easily manipulate the density and composition of culture tissues. Thus, systematic quantifications have become possible and experimental results can be compared with those of analytical and/or computational studies. Finally, for thin sample tissues one can also utilize the recently developed phase-optical imaging technique that renders the mechanical wave activity visible non-invasively [30].

Ironically, some merits of primary cardiac cell cultures are a deficit from other perspectives. For example, some previous studies have considered the thickness of the heart wall and the orientation of cellular alignment along the thickness as important factors in determining the onset of cardiac wave instability [14], [34]–[36]. In the thin quasi-2D layer of cultured cardiac cells, one has no option for addressing these 3D issues. Another important deficit is the existence of various inhomogeneities that are unintentionally introduced during culture preparations. Some of them are quite unavoidable. Another significant factor that should be accounted for in quantifying cardiac wave dynamics in culture is the maturation process of the system: one may consider the culture as a 2D model heart that grows in a controlled environment [30].

The purpose of this paper is to elucidate two commonly observed phenomena that are believed to be caused by the local inhomogeneities of the culture samples that we normally prepare. Firstly, we discuss the phenomenon of spiral wave entrainment that arises at the early stage of cell culture. The entrainment is based on some differences among the rotation periods of neighboring spiral waves and the subsequent drift of the core of the spiral wave tip rotating more slowly. Secondly, we discuss the period-2 oscillatory spiral wave rotation caused by a small set of localized inhomogeneities. We first discuss the observations in experiments and reproduce them in a simple model system incorporating some spatial inhomogeneities.

Our paper is organized as follows. In the next section, we describe the experimental procedure for preparing dissociated cardiac cell cultures and the potential sources for the spatial inhomogeneities. In section 3, we describe the phenomenon of cardiac spiral wave entrainment as typically seen in our experiments. In section 4, we describe the dynamics of a period-2 oscillatory spiral wave as an example of complex oscillatory spiral waves that are made possible by a local inhomogeneity. In section 5, we describe our mathematical model. In section 6, with some arguments based on spatial inhomogeneities, we reproduce the experimental observations in a model system. Section 7 reviews earlier related studies. Finally, we conclude our investigations in section 8.

## 2. Primary cultures of dissociated cardiac cells and spatial inhomogeneities

Confluent dishes of rat ventricle cells are prepared using well-established protocols and procedures described earlier [30, 33]. Typically, ventricles of neonatal (1–2 day old) rats are dissociated with trypsin, counted and plated on 35 mm polystyrene petri dishes that are coated with collagen type IV. Throughout the experiments, the cell density at the time of plating is kept

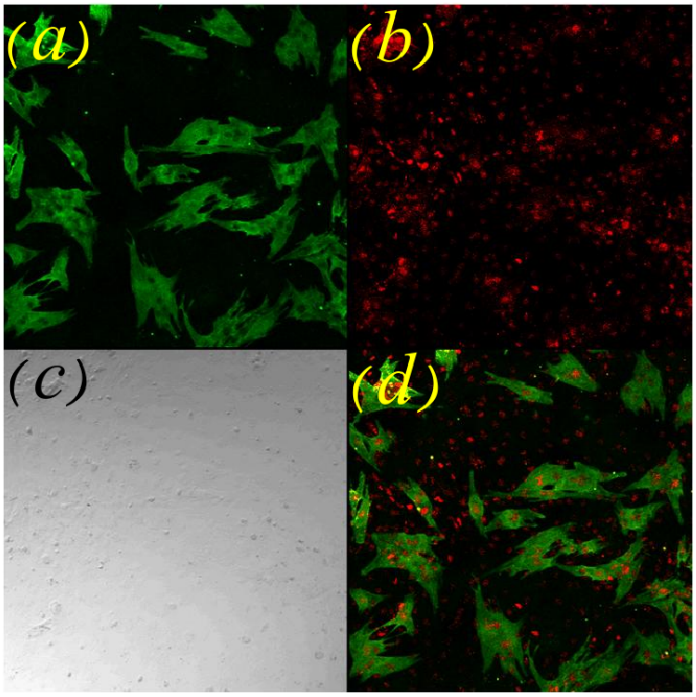


**Figure 1.** Confluent layer of primary culture of dissociated rat ventricular cells: (a) cardiomyocytes rendered visible by myosin immuno-staining (green), (b) nuclei stained by propidium iodide staining (red), (c) a transmitted bright-field image and (d) a superimposed image of (a) and (b). The culture includes two different cell populations, cardiomyocytes and fibroblasts. The nuclei without the myosin filled (green) cell body correspond to fibroblasts. The initial cell density (both types combined) at the time of plating is $2.3 \times 10^3$ cells mm$^{-2}$. The imaging is done at 7 days *in vitro*. The cells are fixed with 4% paraformaldehyde and permeabilized with 0.1% Triton X-100. Then, they are incubated with mouse monoclonal antibodies against cardiac myosin heavy chain (ab15, abcam, Cambridge, UK). The myosin antibodies are tagged by fluorescein-labeled isothiocyanate (FITC) conjugated secondary antibody (green) and the nuclei are stained with 2 $\mu$g ml$^{-1}$ propidium iodide (red). Each frame is $640 \times 640$ $\mu$m$^2$.

at $2.3 \times 10^3$ cells mm$^{-2}$. Individual cardiac cells are randomly oriented at the time of plating, therefore there is no directional anisotropy in the system unlike in real heart tissue in which rod-shaped cardiomyocytes are aligned along their long axes in a non-trivial way. This property seems to be maintained even in the mature stage of the culture (see figure 1): cardiomyocytes are dispersed randomly and their long axes have no directional preference.

Another feature of our *in vitro* cardiac tissue is that it is composed not only of cardiomyocytes but also of fibroblasts. As figure 1 well illustrates, during a mature stage of the culture fibroblasts and cardiomyocytes are inter-dispersed with each other forming a confluent layer (see figure 1(d)). Quite a significant fraction of the total area is covered by fibroblasts. Here, the density of the fibroblast cell population is higher than the physiologically relevant value: this is because at this developmental stage, fibroblasts still replicate while cardiomyocytes do not. Therefore, the ratio of the densities of the two different cell populations is likely to vary

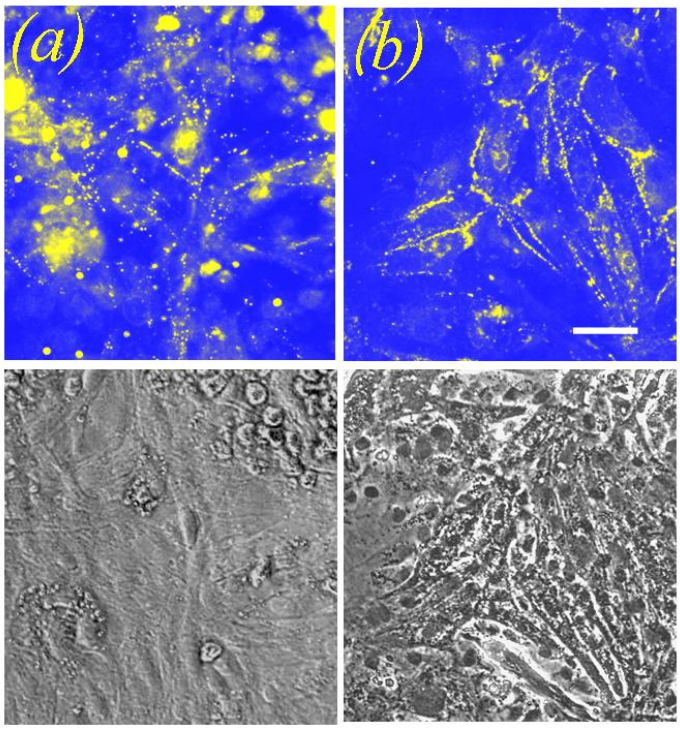


**Figure 2.** Gap junction expression in primary culture of dissociated rat ventricular cells at 6 days *in vitro* (a) and 13 days *in vitro* (b). Top row shows images with connexin-43 immuno-staining (yellow) and the bottom row shows the corresponding phase contrast images (scale bar: 50 $\mu$m). The initial cell density (both types combined) at the time of plating is $2.3 \times 10^3$ cells mm$^{-2}$. Fixed and permeabilized ventricular cells are incubated with rat connexin-43 (Sigma, St Louis, MO, USA) primary antibody. The connexin-43 primary antibodies are tagged by FITC conjugated secondary antibodies. Gap-junction proteins are expressed by small yellow speckles, while the large yellow blobs are non-specifically tagged cell bodies.

gradually over days. Taking all these facts together, we may state that the culture medium is not an ideal, homogeneous, isotropic tissue: it is neither homogeneous nor isotropic at various levels. The size of spatial inhomogeneity can be as large as a few millimetres.

The existence of spatial inhomogeneity is especially evident during the first few days after cell plating. At this stage, cells tend to form small aggregates not fully attached to the substrate (see figure 2(a)). These small cell aggregates progressively smear out themselves on to the substrate forming a thin tissue as the system becomes more mature in time (see figure 2(b)). Consequently, the effective density of cardiomyocytes participating in the *in vitro* tissue sitting right on the substrate may be viewed to increase gradually over several days after the initial plating. While this happens, the density of gap junction proteins on the plasma membrane, which mediate direct myocyte–myocyte connectivity, increases as well (see figure 2(b)). In other words, the degree of electrical connectivity among neighboring myocytes also increases with time.

## 3. Early developmental stage: spiral wave entrainment

In almost all culture dishes that we have prepared, some noisy wave activities emerge spontaneously, often as early as one day after the initial cell plating as shown in figure 3. We believe that excitable ventricle cells can spontaneously beat by themselves under some culture conditions and initiate wave activities. Alternatively, some pacemaker cells (e.g. from the atrioventricular node) may be unintentionally included in our cell cultures, and they may have initiated waves. Given the fact that every culture plate that we have prepared produces wave activities spontaneously, the first scenario seems more plausible.

With time passing by, larger cardiac wavelets emerge increasingly more frequently. Then, they interact with each other as they propagate in the active medium. Considering the fact that the overall gap junction expression is quite low as shown in figure 2 and that many cardiomyocytes form small localized aggregates at the early stage (1–3 days *in vitro*), not being fully integrated into the bulk tissue, the emergence of these sizable wavelets having a quite well-defined characteristic length scale is surprising.

As the culture becomes mature, each broken wavelet usually becomes a small pair of spirals. Neighboring spiral waves then compete and entrain each other, and in the end only a few spiral cores dominate the entire culture medium (figure 3). Figure 4 details this entrainment behavior: one of the three spiral cores within the red circle mark in figure 4(a) has disappeared in figure 4(b), and similarly one of the two in figure 4(b) is removed in figure 4(c). The sequence of images in figure 5 further details the transition from the state shown in figure 4(b) to that in figure 4(c). Initially, there are two spiral wave cores that are co-rotating, exchanging their arms at every turn (see figure 5(a) and (b)). At one instance, one of the spiral tips (traced by the blue line) is suddenly 'displaced' (figure 5(c)) and the co-rotating symmetry of the pair is broken. Subsequently, the displaced one drifts rapidly away from the other in the form of a pulled spring and exits from the field of view. The displacement of one of two spiral tips may be viewed as the transition of a spiral core that faces an increasing limitation on space and time for a curling.

As will be discussed more in detail later in the section on model studies, the spiral wave core entrainment seems primarily due to a slight difference in the rotation periods of two neighboring spiral waves. The annihilation zone where two traveling wave fronts meet and annihilate progressively moves toward the core of the slowly rotating spiral wave (see e.g. [37]). Then, when the annihilation zone becomes so close to the slower spiral core, the tip suddenly starts to drift. The rotation periods of spiral waves in a given medium can be different because spiral cores are often pinned to a different localized inhomogeneity, and the rotation period can vary according to the size of the inhomogeneity (see for example, [38]–[40]).

## 4. Localized inhomogeneities and 2 : 1 oscillatory spiral reentry wave

Another important phenomenon that is believed to be caused by a localized inhomogeneity in the culture medium is meandering spiral waves that drive a complex-oscillatory excitation rhythm. This was discussed in our earlier report [33] and one of them is given in figure 6: the sequence of images illustrates a spiral tip traveling along a closed orbit that is composed of two loops, one small and the other larger. As the wave tip rotates along the two different loops (see figure 6(b)), the amplitudes and intervals of successive beats alternate between two different values in the bulk medium: one example is the time series (red line in figure 6(c)) acquired at the position marked by a red dot in figure 6(a). This period-2 oscillatory state lasts for quite

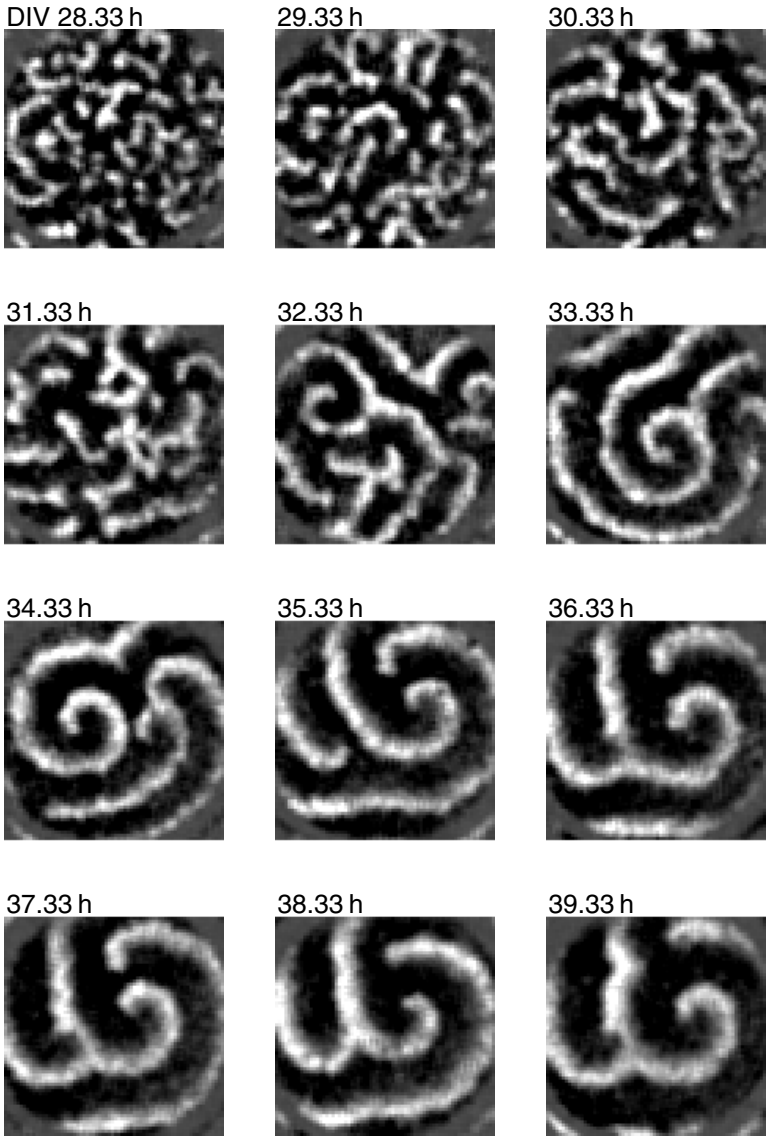


**Figure 3.** A typical spatiotemporal evolution of spiral waves in the early stage of a primary culture of dissociated rat ventricular cells: generically, many small wavelets compete with each other and a few spiral cores survive at the end. The electro-mechanical activity of the culture tissue is visualized by the propagation-induced phase contrast macroscope and image processing software developed earlier by us (for details, see [30]). Each frame is $35 \times 35\,\mathrm{mm}^2$.

some time until it suddenly switches to a different oscillatory state (see [33] for details). Note that inside the larger lobe (i.e. the position marked by a green dot in figure 6(a)), cells are fully excited only once during each period-2 cycle oscillation of the bulk medium (see the time series (green) in figure 6(c)). This period-2 oscillatory spiral reentry distinguishes itself from similar period-2 oscillatory spiral structures that naturally arise in period-2 oscillatory homogeneous media by the fact that it has no 'line defect' attached to its core [41]–[43].

We believe that the unusually shaped spiral tip orbit and the resulting dynamics are supported by the presence of a local inhomogeneity as we will recapitulate the same

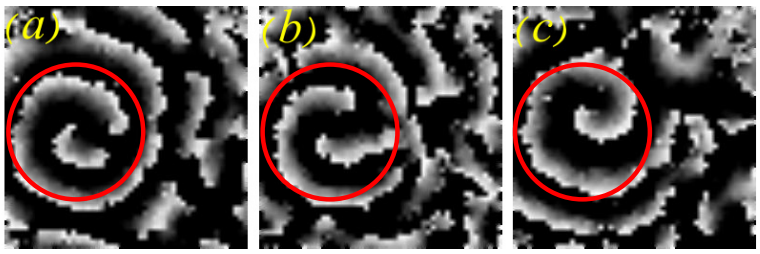


**Figure 4.** Snapshot images illustrating the reduction in the number of spiral cores in the primary of culture of dissociated rat ventricular cells: (a) 42 h *in vitro*, (b) 44 h *in vitro* and (c) 3860 ms after the state shown in (b). The field of view is $20 \times 20\,\mathrm{mm}^2$.

phenomenon in the section for model simulations. Although unusual meandering spiral tip trajectories are known to exist in homogeneous excitable media [44]–[46], so far none of them exhibits a frequency-locked behavior such as the period-2 oscillation that we discuss here. Frequency-locked meandering orbits are known to exist only when the concerned medium has spatial anisotropy [47] or has a localized extrinsic perturbation [48]. This fact suggests that our observation is very likely due to some localized inhomogeneities. In the following sections, we explain how localized inhomogeneities can cause the observed phenomena.

## 5. Model

The aforementioned two experimental observations can be well reproduced in computer simulations of a cardiac tissue model that incorporates some realistic spatial heterogeneities. Basically, we use the three variable simplified model of heart tissue that was developed by Fenton and Karma [34]. The Fenton–Karma model, although it does not involve detailed ion channel properties explicitly, is well known for its faithful reproduction of the action potentials in the myocytes of several different animals. Since we are interested in the qualitative behaviors of the cardiac spiral waves interacting with localized inhomogeneities, this, qualitative, yet physiologically relevant, model seems just appropriate.

In the model, the transmembrane potential is determined by three ionic currents, which are the fast inward current $I_{\mathrm{fi}}$, the slow outward current $I_{\mathrm{so}}$ and the slow inward current $I_{\mathrm{si}}$. The equation for the membrane potential can be written as follows.

$$\frac{\partial V(\mathbf{x},t)}{\partial t} = D\nabla^2 V(\mathbf{x},t) - [I_{\mathrm{fi}}(V,v) + I_{\mathrm{so}}(V) + I_{\mathrm{si}}(V,w)]/C_{\mathrm{m}}. \tag{1}$$

The ionic currents have the following mathematical form.

$$I_{\mathrm{fi}} = -vp(V-V_{\mathrm{c}})(1-V)/\tau_{\mathrm{d}},$$

$$I_{\mathrm{so}} = V(1-p)/\tau_0 + p/\tau_{\mathrm{r}},$$

$$I_{\mathrm{si}} = -w[1+\tanh\{k(V-V_{\mathrm{c}}^{\mathrm{si}})\}]/(2\tau_{\mathrm{si}}).$$

Two gating variables $v$ and $w$ are described by

$$\frac{\partial v(\mathbf{x},t)}{\partial t} = (1-p)(1-v)/\tau_v^-(V) - pv/\tau_v^+(v), \tag{2}$$

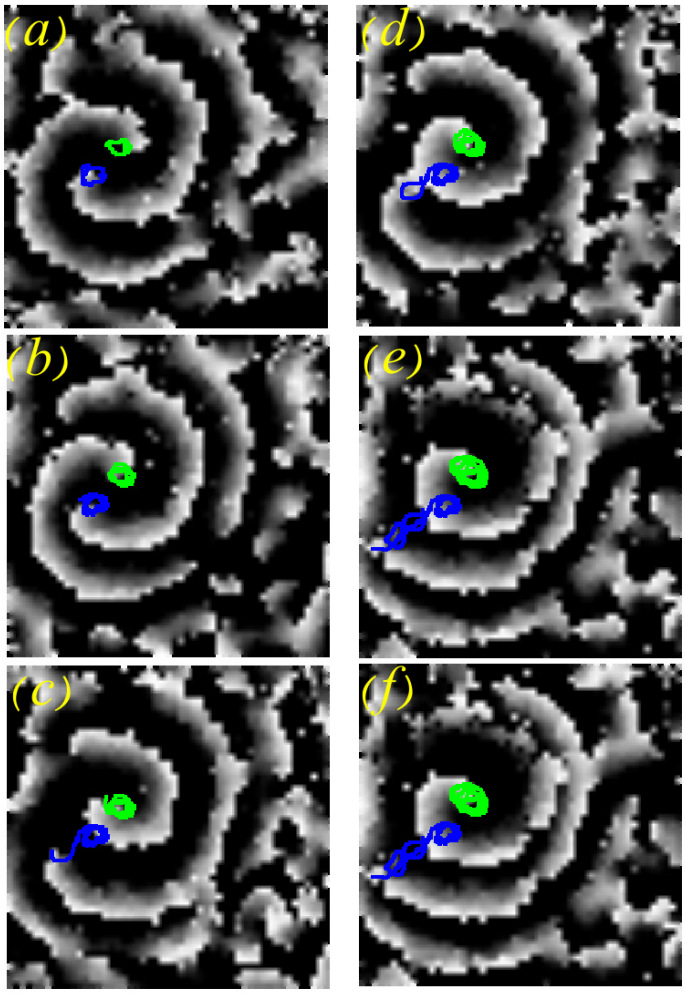


**Figure 5.** Two competing spiral cores and a subsequent drift of one core. The two spiral cores are rotating periodically about their tips, tracing more or less a circle ((a) $t = 0$ and (b) $t = 560$ ms). The positions of both spiral tips are traced manually and colored in blue and green, respectively. They exchange their arms once in each rotation. One of them suddenly starts to drift off from its circular orbit in (c) $t = 640$ ms. Subsequently, the blue trace rapidly moves away from the circular orbit in the form of a pulled spring (see (d) $t = 720$ ms, (e) $t = 840$ ms, and (f) $t = 1400$ ms).

$$\frac{\partial w(\mathbf{x}, t)}{\partial t} = (1-p)(1-w)/\tau_w^-(V) - pw/\tau_w^+(v), \tag{3}$$

where $\tau_v^- = (1-q)\tau_{v1}^-(V) + q\tau_{v2}^-(V)$ and

$$p = \begin{cases} 1 & \text{if } V \geqslant V_c \\ 0 & \text{otherwise,} \end{cases} \qquad q = \begin{cases} 1 & \text{if } V \geqslant V_v \\ 0 & \text{otherwise.} \end{cases}$$

$\tau_d$, $\tau_0$, $\tau_r$, $\tau_{si}$, $\tau_{v1}^-$, $\tau_{v2}^-$, $\tau_v^+$, $\tau_w^-$ and $\tau_w^+$ are various characteristic time constants.

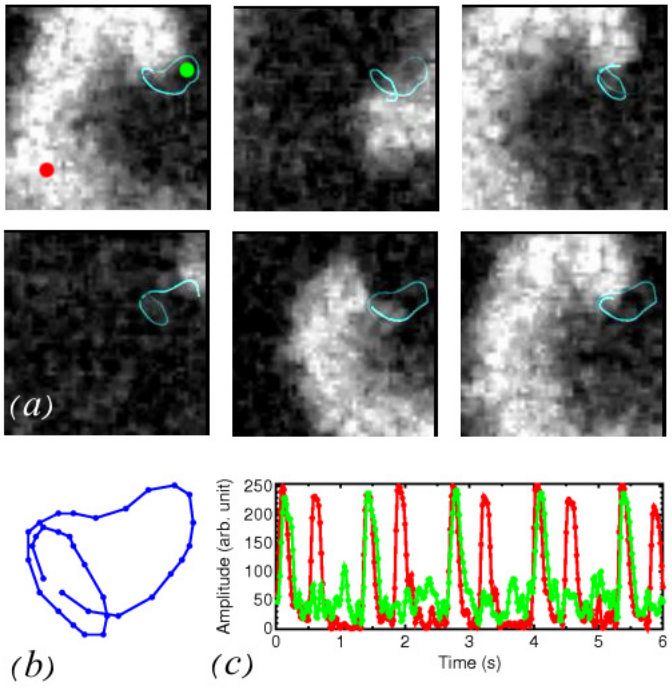


**Figure 6.** A spiral tip rotating around a two-lobe orbit: (a) a sequence of snapshot images taken at six different phases ($t = 0, 240, 580, 820, 1200$ and 1300 ms, sequentially from left to right and top to bottom), (b) a blown-up image of the complete two-lobe orbit traced by the spiral tip and (c) two local time series acquired at two different locations marked by dots in (a) $t = 0$. The graded blue lines in (a) mark the location of the tip during the past 1000 ms. The field of view is $7.8 \times 7.8\,\mathrm{mm}^2$. The culture is 5 days *in vitro*.

In order to mimic the spatial inhomogeneities of our culture tissues, some heterogeneities are added to the above model as described in the next section. Basically, we consider two different cases: firstly, randomly distributed small-size heterogeneities and secondly, a pair of neighboring obstacles whose dimension is comparable to that of spiral wave core.

We have used the forward Euler method to integrate the cable equation (1) and equations for two gating variables (2) and (3). The integration time step $\Delta t$ is 0.05 ms and the grid size $\Delta x$ is 0.05 cm. The diffusion constant $D$ is $0.001\,\mathrm{cm}^2\,\mathrm{ms}^{-1}$ unless otherwise mentioned, and $C_\mathrm{m} = 1\,\mu\mathrm{F\,cm}^{-2}$. The system size is $256 \times 256$ (or in real physical dimensions, $12.8 \times 12.8\,\mathrm{cm}^2$) unless otherwise specified.

## 6. Simulation results

### *6.1. Local inhomogeneities, core anchoring and spiral wave entrainment*

Localized spatial inhomogeneities (anatomical obstacles) are often discussed as a source for cardiac reentry generation [49]–[52]. Another well known phenomenon associated with small obstacles is that rotating spiral wave cores can be attracted to them and get pinned [38], [53]–[55]. Since spiral reentry dynamics is a critical factor governing the overall dynamics of

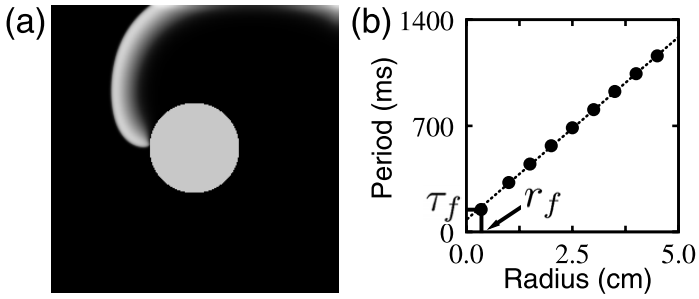


**Figure 7.** An anchored spiral wave rotating around a non-conductive disk zone (gray) in a Fenton–Karma model simulation in (a) and its period as a function of the obstacle radius in (b). The $V$-field of the model is rendered in gray scale in (a). The rotation period of the spiral wave in (a) is 568 ms and the radius of the obstacle is 2.0 cm. The free running spiral core rotates around a circular orbit of radius $r_f = 0.35$ cm with a rotation period $\tau_f = 148.1$ ms (in (b), only the radius of obstacle $\geqslant r_f$ is considered). The parameter values are $\tau_v^+ = 3.33$, $\tau_{v_1}^- = 19.6$, $\tau_{v_2}^- = 1000$, $\tau_w^+ = 667$, $\tau_w^- = 11$, $\tau_d = 0.420$, $\tau_0 = 8.3$, $\tau_r = 50$, $\tau_{si} = 45$, $k = 10$, $V_c^{si} = 0.85$, $V_c = 0.13$ and $V_v = 0.055$, respectively.

the whole system, it is important to understand how pinning (or depinning) takes place and how their physical properties modify the dynamics of spiral waves.

According to the numerical simulation study by Zou *et al* [38], the pinning–depinning transition depends on two factors, the radius of the obstacle and the 'impact parameter.' Interestingly, in the phase space of these two parameters, the critical line separating the trapped and the untrapped goes through the origin suggesting that the critical radius for the trapping could be very small.

The conduction velocity and rotation period of a pinned spiral wave are different from those of a free-running spiral wave, since the different curvature of a (round) obstacle imposes a different source–sink relation near the core [54]. Some careful measurements on this issue were recently made by Lim *et al* [55] who have used cultured cardiac tissues having a disk-shaped obstacle. Their study seems focused at the nonlinear regime in which there exists a strong conduction velocity dispersion effect.

In order to make a simple explanation of our experimental observations, here we only consider the case when the size of the obstacle is rather big (i.e. larger than the size of the circular orbit traced by the tip of an unpinned spiral wave in an homogeneous medium). One immediate consequence of the pinning, then, would be period lengthening [40]: in this 'linear regime' the conduction velocity does not change much (i.e. conduction velocity dispersion is very weak); therefore the anchored spiral tip simply travels a longer circumference in order to complete a full rotation.

Simulations on the Fenton–Karma model with a large obstacle well support this picture (see figure 7): the rotation period increases linearly as a function of the peripheral length of the non-conducting zone when a disk is considered as an obstacle (see figure 7). The spiral tip is moving at a constant speed regardless of the size of the obstacle, and this is natural since the wave dispersion becomes irrelevant for a fully recovered medium.

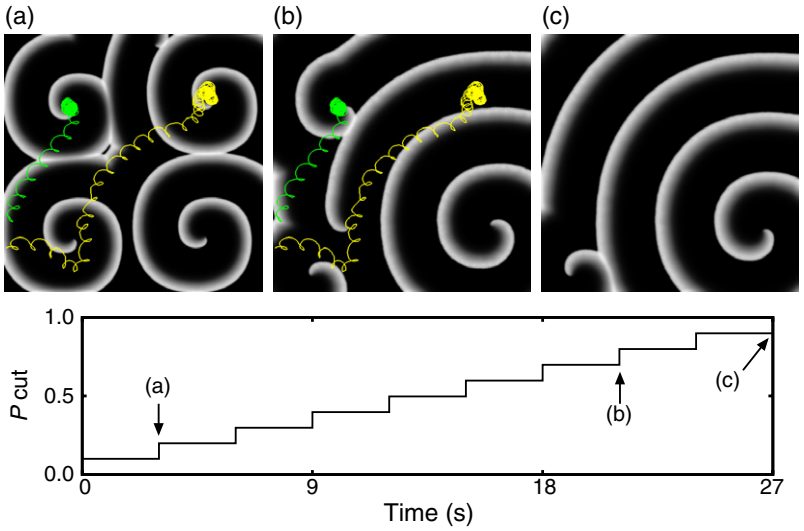


**Figure 8.** Competition of four spiral waves in an evolutionary, heterogeneous, Fenton–Karma model. The images (a)–(c) are snapshots acquired at the marked locations ($\bar{p} = 0.1, 0.7$ and $0.9$, respectively) in the plot of $\bar{p}$ versus time, respectively. The superimposed lines in (a) and (b) mark the traces of two spiral cores that have drifted out of the field of view. The parameter values are $\tau_v^+ = 3.33$, $\tau_{v_1}^- = 19.6$, $\tau_{v_2}^- = 1000$, $\tau_w^+ = 667$, $\tau_w^- = 11$, $\tau_d = 0.420$, $\tau_0 = 8.3$, $\tau_r = 50$, $\tau_{si} = 45$, $k = 10$, $V_c^{si} = 0.85$, $V_c = 0.13$ and $V_v = 0.055$, respectively.

Excitable media such as cultured cardiac tissue naturally involve various localized inhomogeneities. Therefore, in such media several spiral cores, each of which have a quite different rotation period, can co-exist simultaneously. However, these spirals will compete with each other for their territories and eventually the one having the highest rotation frequency will overtake the slower ones and dominate the system (see, e.g. [37]).

The anchoring of spiral wave cores and the subsequent period lengthening of the spiral waves discussed above are believed to be relevant to the entrainment dynamics in the early stage of the tissue development that is addressed in section 3 (see figure 3 and 4). Yet, the typical length scale of spatial inhomogeneities in our cultures can be much smaller than the full extension ($\sim$2 mm) of a normal circular tip trajectory. Then, the aforementioned anchoring phenomenon becomes irrelevant to the actual entrainment dynamics. However, even when there are randomly distributed small inhomogeneities, some small differences can exist among the rotation periods of different spiral waves, thus a similar competition based on the rotation period ensues. Such a case is considered in figure 8.

For the simulation results shown in figure 8, each pixel is assigned one of two different levels of diffusivity ($D = 0.001$ or $0.002\,\mathrm{cm^2\,ms^{-1}}$) in a random fashion in order to mimic the overall spatial inhomogeneity in actual *in vitro* cardiac tissue. A sequence of random numbers $p$ ranging from 0 to 1 is generated based on an uniform deviate, and they are assigned to different pixels. Then, for a given threshold $p_{cut}$, only pixels with $p < p_{cut}$ are assumed to have $D = 0.002\,\mathrm{cm^2\,ms^{-1}}$. Other pixels having $p > p_{cut}$ are assumed to have $D = 0.001\,\mathrm{cm^2\,ms^{-1}}$. This simple model reflects the fact that for the early stages of cardiac cell cultures the myocyte population density is not uniform and that the *in vitro* culture tissue is composed of two

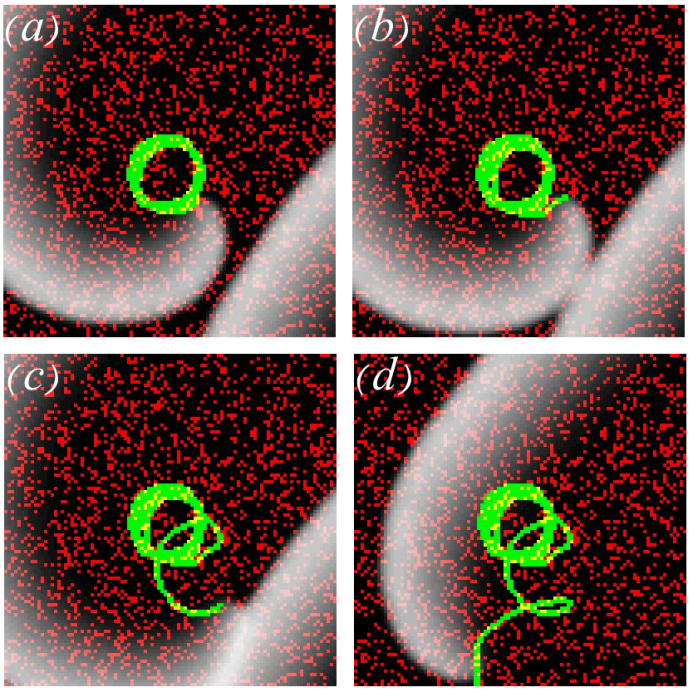


**Figure 9.** A close-up view of the onset of the drift of a spiral core shown in figure 8(b). The red (black) pixels have $D = 0.002(0.001)\,\mathrm{cm^2\,ms^{-1}}$. The green line is the trace of the tip of spiral wave (in gray scale). $t = 0, 0.8, 1.6$ and 2.1 sec for (a)–(d), respectively. The spiral core starts to drift when the wave from the lower right-hand corner invades too close to the tip.

different types of cells, myocytes and fibroblasts. Thus, one may view the pixels having $D = 0.002\,\mathrm{cm^2\,ms^{-1}}$ as representing a small patch of well connected myocytes, whereas the pixels having $D = 0.001\,\mathrm{cm^2\,ms^{-1}}$ represent an immature network of myocytes or network of fibroblasts. Finally, the threshold value $p_{\mathrm{cut}}$ is increased in time to reflect the developmental process taking place in the *in vitro* tissues: the value of $p_{\mathrm{cut}}$ is increased from 0.1 to 0.9 with a step size of 0.1 to simulate that the portion of mature cells and/or the cell-to-cell connectivity increases in time.

The particular example depicted in figure 8(a) shows four different spirals initially. Their periods are slightly different because the corresponding spiral tips experience a different landscape of inhomogeneities. Shock zones where waves from different spiral cores collide and annihilate form, and they progressively move toward the cores of the slowly rotating spiral waves (not shown). When a shock zone reaches too close to the slow spiral wave tip, beyond a critical value, the circular motion of the slow tip can no longer be supported and the orbit drifts off toward the system boundary and exits from the field of view. Note that when the system has evolved to the state shown in figure 8(c), only two spiral cores remain.

The underlying spatial inhomogeneities and the very onset of a spiral core drift is detailed in figure 9. We note that the orbit traced by the spiral tip, even before the major drift starts, has some noticeable wobbles. In other words, it does not repeat itself exactly along a circle. This minor drift of an inherently circular trajectory is due to the presence of small scale inhomogeneities, and we note that one of the earlier numerical studies addressing spiral wave

competition [39] confirmed that such small fluctuations can provide spatial dependence to the frequency of spiral waves and form the formation of a dominant spiral. We note that the major drift motion is triggered only when there is a direct interaction of the core with the incoming wave fronts.

### *6.2. Spiral reentry wave with two alternating periods*

Some complex-oscillatory beatings can be supported in *in vitro* cardiac tissues due to the presence of a meandering spiral reentry. Even in perfectly homogeneous excitable media, meandering spiral tip dynamics forming an epicycloid or cycloid orbit can emerge through a Hopf bifurcation of a (circular) simply rotating spiral wave [44, 45]. However, no case of frequency-locked meandering is known to exist so far in homogeneous media. In other word, no complex periodic cycle is likely to occur in a regular homogeneous excitable medium. With this fact in mind, we demonstrate that the meandering of the cardiac reentry wave shown in figure 6, producing a period-2 cycle oscillation in the bulk medium, can be caused by the presence of a simple pair of localized inhomogeneities: one of them is an absolute (conduction) obstacle, while the other is a functional obstacle that has a prolonged recovery period.

Figure 10 illustrates the pair of obstacles located neighboring each other and the sequential images of a spiral reentry rotating about it at different instances of time. The disk domain labeled by **B** in figure 10(e) represents an absolute obstacle through which no wave can conduct. Since its physical dimension is set sufficiently large enough, a spiral tip can be anchored and pinned to it as discussed in figure 7. Without the functional obstacle labeled by **A**, the pinned spiral wave would have been stably circulating about the disk shaped domain **B** in a trivial fashion. The additional obstacle **A**, which is functional, works as a 'valve' allowing the spiral tip to pass through only every other time. In other words, the additional obstacle acts as a 2 : 1-block obstacle. This can be achieved by making the region have a longer action potential duration (i.e. lengthening the recovery period). With this functional 2 : 1-block obstacle in place, the spiral tip traces out a closed two-lobe meandering orbit in a periodic manner—along orbit-1 followed by orbit-2 (see figure 10(a)–(d)). This alternating cycle repeats and drives a period-2 cycle excitation in the bulk medium as shown in the return map of the successive inter-beat-intervals $T_n$ (see figure 10(f)).

The physical dimensions (the sizes and shapes) of the conduction obstacles are not a critical factor in generating the closed period-2 orbit, as long as they are properly adjusted, the spiral core will stay around the pair of conduction obstacles. One important factor is that the physical dimension of the 2 : 1-block obstacle must not be too large, otherwise the spiral core cannot be 're-injected' to the disk-shaped absolute conduction obstacle and subsequently a closed period-2 cycle would not be feasible.

## 7. Discussion

The drift (or complex trajectory) of a spiral reentry core that is caused either by its interaction with a higher frequency source (pacing) or by some extrinsic gradient field is a well established problem in the scientific community studying excitable wave dynamics. The phenomenon was first discussed in connection with spiral waves in Belousov–Zhabotinsky chemical systems [56, 57] and later discussed in other systems such as *Dictyostelium discoidium* amoeba populations [11] and cardiac tissues [58]–[61] as well. There also exist several numerical

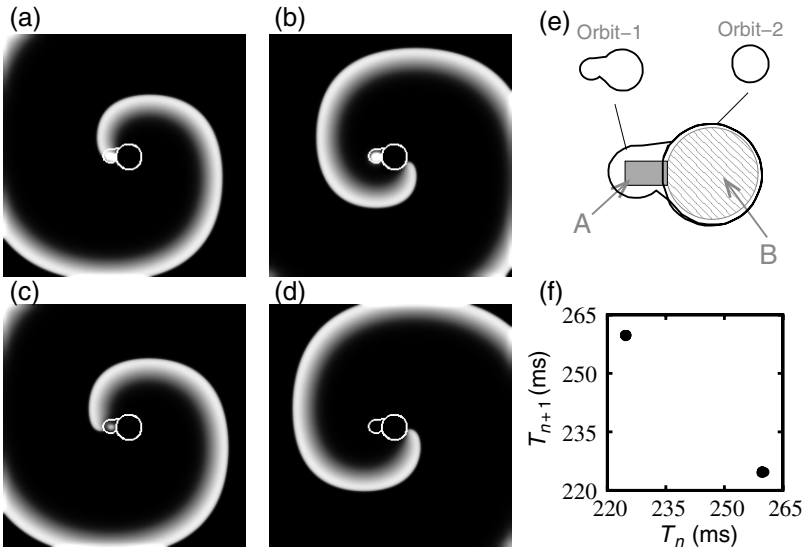


**Figure 10.** An anchored spiral wave rotating around a pair of conduction obstacles (**A**: 2 : 1-block obstacle, **B**: absolute conduction obstacle). (a) The region **A** is excited as the core passes. (b) The tip has moved on to the absolute conduction obstacle **B**. (c) The 2 : 1-block obstacle has not fully recovered from its previous excitation, and the spiral tip moves around the obstacle **A**. (d) The tip has moved on to the obstacle **B** again and completes a cycle. The complete orbit (orbit **1** + orbit **2**) traced out by the tip around the pair of conduction obstacles is given in (e). (f) Return map of successive inter-beat-intervals $T_n$. The parameter values for the bulk medium are: $\tau_v^+ = 3.33$, $\tau_{v_1}^- = 19.6$, $\tau_{v_2}^- = 1000$, $\tau_w^+ = 667$, $\tau_w^- = 11$, $\tau_d = 0.410$, $\tau_0 = 8.3$, $\tau_r = 50$, $\tau_{si} = 45$,$k = 10$, $V_c^{si} = 0.85$, $V_c = 0.13$, $V_v = 0.055$. For region **A**, $\tau_v^+ = 3.33$, $\tau_{v_1}^- = 15.6$, $\tau_{v_2}^- = 5$, $\tau_w^+ = 350$, $\tau_w^- = 80$, $\tau_d = 0.400$, $\tau_0 = 1000$, $\tau_r = 2000$, $\tau_{si} = 13$, $k = 15$, $V_c^{si} = 0.45$, $V_c$=0.15, $V_v = 0.04$. The diffusivity constant $D$ is zero for region **B** and $0.001\,\mathrm{cm}^2\,\mathrm{ms}^{-1}$ for the other region. The geometry of region **A** is $0.5 \times 0.25\,\mathrm{cm}^2$ and the radius of region **B** is 0.6 cm.

studies based on reaction–diffusion models regarding spiral drift phenomena [37, 39, 40, 48, 58, 62]. However, the topic still remains an area of active research, in particular in cardiology: for example, anti-tachycardia pacing, which eliminates spiral waves, has a wide clinical use but its mechanism is still not well understood. This is in part due to the fact that studying the phenomenon of spiral core drift in an intact heart involves several difficult challenges as mentioned earlier.

Our current report is one of very few cases that directly demonstrate spiral wave drift taking place in a cardiac system. In fact, only last year Agladze *et al* [60] quantified a similar cardiac wave drift phenomenon for the first time in a system that is very similar to ours. In their study, the drift was induced by a fast-paced, extrinsic stimulation, while in our system the drift was a consequence of two competing spiral waves having slightly different rotation periods.

Along with the drift phenomenon, the interaction of spiral reentries with anatomical obstacles has been another important topic in excitable wave dynamics. For example, the pinning–depinning transition in the presence of a gradient field was studied numerically by

Zou *et al* [38]. Their study was motivated by the fact that the pinning phenomenon can be quite important in cardiology since the myocardium is replete with small inhomogeneities. In fact, it is known that the arrest of a meandering spiral, for example, can result in a simpler monomorphic 'flutter-like' activity [54]. Quite recently L Tung's group conducted a set of careful measurements on the relationship between the size of obstacle and the conduction velocity (or rotation period) of attached spiral waves, and their detachments following a reduction in excitability [55].

The majority of previous investigations on the effect of local spatial heterogeneities on cardiac spiral wave dynamics has focused on the pinning effect. Here, our study has demonstrated that the localized obstacles are not just a pinning site but a proper arrangement of them can confer a regular, yet non-trivial (e.g. alternans-like) beating rhythm to the bulk tissue. The rhythm can become more complex as the geometry of the set of small obstacles, to which the spiral tip is anchored, has more complex twists and turns [33].

## 8. Conclusion

Using computer simulations on a simple physiological model, we have reproduced two recurring generic phenomena that are repeatedly observed in our *in vitro* cardiac wave experiments, namely, the spiral wave entrainment (drift) dynamics and the complex-oscillatory meandering spiral waves. The key to this success is that our model simulations incorporate some simple, yet realistic, spatial inhomogeneities of the cultured tissue.

The primary cultures of ventricular cells that we have used for cardiac wave experiments include fibroblasts as well as myocytes. Abrupt discontinuities exist at the cellular interfaces between myocytes and fibroblasts: electrical impulses can conduct through a sizable bridge of fibroblasts between cardiomyocytes, yet at much slower speed [63, 64]. Therefore, the very existence of fibroblasts and their spatial distribution in confluent culture tissue should be accounted for. In other words, the two observed phenomena originate basically from the modulations in the path-lengths and periods of spiral tips, when the modulations are caused by the existence of local heterogeneities (e.g. varying cell density of myocytes and fibroblasts).

Knowing that localized heterogeneities are common in diseased hearts, the discussed phenomena not only pertain to *in vitro* tissues but are also relevant to many cases in clinical cardiology. We point out that post-myocardial infarction ventricles can have multiple reentrant paths and reentries often share the paths forming different orbits [49]–[52].

## Acknowledgments

This work is supported by Doyak project (R17-2007-017-01000-0) of the Korea Ministry of Science and Technology. T Y Kim is supported by Seoul Science Fellowship.

## References

[1] Swinney H L and Krinsky V I (ed) 1992 *Waves and Patterns in Chemical and Biological Media* (Amsterdam: North-Holland)
[2] Kapral R and Showalter K (ed) 1995 *Chemical Waves and Patterns* (Dordrecht: Kluwer)
[3] Vanag V K and Epstein I R 2001 *Science* **294** 835
[4] Castets V, Dulos E, Boissonade J and De Kepper P 1990 *Phys. Rev. Lett.* **64** 2953

[5] Ouyang Q and Swinney H L 1991 *Nature* **352** 610
[6] Lee K J, McCormick W D, Pearson J E and Swinney H L 1994 *Nature* **369** 215
[7] Lee K J and Swinney H L 1995 *Phys. Rev.* E **51** 1899
[8] Li G, Ouyang Q, Petrov V and Swinney H L 1996 *Phys. Rev. Lett.* **77** 2105
[9] Etrl G 1991 *Science* **254** 5039
[10] Beta C, Moula M G, Mikhailov A S, Rotermund H H and Ertl G 2004 *Phys. Rev. Lett.* **93** 188301
[11] Lee K J, Cox E C and Goldstein R E 1996 *Phys. Rev. Lett.* **76** 1174
[12] Pálsson E, Lee K J, Goldstein R E, Franke J, Kessin R H and Cox E C 1997 *Proc. Natl Acad. Sci. USA* **94** 13719
[13] Sawai S, Thomason P A and Cox E C 2005 *Nature* **433** 323
[14] Winfree A T 1994 *Science* **266** 1003
[15] Karma A 1994 *Chaos* **4** 461
[16] Glass L 1996 *Phys. Today* **49** 40
[17] Gray R A, Pertsov A M and Jalife J 1998 *Nature* **392** 75
[18] Lechleiter J, Girard S, Peralta E and Clapham D 1991 *Science* **252** 123
[19] Miyazaki S, Yuzaki M, Nakada K, Shirakawa H, Nakanishi S, Nakade S and Mikoshiba K 1992 *Science* **257** 251
[20] Newman E A 2001 *J. Neuroscience* **21** 2215
[21] Dumollard R, Carroll J, Dupont G and Sardet C 2002 *J. Cell Sci.* **115** 3557
[22] Davidenko J M, Kent P F, Chialvo D R, Michaels D C and Jalife J 1990 *Proc. Natl Acad. Sci. USA* **87** 8785
[23] Witkowski F X, Leon L J, Penkoske P A, Giles W R, Spano M L, Ditto W L and Winfree A T 1998 *Nature* **392** 78
[24] Weiss J N, Garfinkel A, Karagueuzian H S, Qu Z and Chen P-S 1999 *Circulation* **99** 2819
[25] Weiss J N, Chen P-S, Qu Z, Karagueuzian H S and Garfinkel A 2000 *Circ. Res.* **87** 1103
[26] Baker L C, London B, Choi B R, Koren G and Salama G 2000 *Circ. Res.* **86** 396
[27] Bub G, Glass L, Publicover N G and Shrier A 1998 *Proc. Natl Acad. Sci. USA* **95** 10283
[28] Bub G, Shrier A and Glass L 2002 *Phys. Rev. Lett.* **88** 058101
[29] Iravanian S, Nabutovsky Y, Kong C R, Saha S, Bursac N and Tung L 2003 *Am. J. Physiol. Heart Circ. Physiol.* **285** 449
[30] Hwang S-m, Yea K-h and Lee K J 2004 *Phys. Rev. Lett.* **92** 198103
[31] Bursac N, Aguel F and Tung L 2004 *Proc. Natl Acad. Sci. USA* **101** 15530
[32] Bien H, Yin L and Entcheva E 2006 *Biophys. J.* **90** 2628
[33] Hwang S-m, Kim T Y and Lee K J 2005 *Proc. Natl Acad. Sci. USA* **102** 10363
[34] Fenton F and Karma A 1998 *Chaos* **8** 20
[35] Ou Z, Kil J, Xie F, Garfinkel A and Weis J N 2000 *Biophys. J.* **78** 2761
[36] Alonso S, Saqués F and Mikhailov A S 2003 *Science* **299** 1722
[37] Lee K J 1997 *Phys. Rev. Lett.* **79** 2907
[38] Zou X, Levine H and Kessler D 1993 *Phys. Rev.* E **47** 800
[39] Hendrey M, Ott E and Antonsen Jr T M 1999 *Phys. Rev. Lett.* **82** 859
[40] Xie F, Qu Z, Weiss J N and Garfinkel A 2001 *Phys. Rev.* E **63** 031905
[41] Goryachev A, Chaté H and Kapral R 1998 *Phys. Rev. Lett.* **80** 873
[42] Park J-S and Lee K J 1999 *Phys. Rev. Lett.* **83** 5393
[43] Kim T Y, Woo S-J, Hwang S-m, Hong J H and Lee K J 2007 *Proc. Natl Acad. Sci. USA* **104** 11639
[44] Barkley D 1994 *Phys. Rev. Lett.* **72** 164
[45] Li G, Ouyang Q, Pertov V and Swinney H L 1996 *Phys. Rev. Lett.* **77** 2105
[46] Fenton F H, Cherry E M, Hastings H M and Evans S J 2002 *Chaos* **12** 852
[47] Roth B J 1998 *Phys. Rev.* E **57** 3735
[48] Hwang S-m, Choe W-G and Lee K J 2000 *Phys. Rev.* E **62** 4799
[49] Lazzara R and Scherlag B J 1988 *Am. J. Cardiol.* **15** 20

[50] Stevenson W G, Friedman P C, Sager P T, Saxon C A and Pavri B 1998 *Circulation* **98** 308
[51] Schalij M J, Boersma L, Huijberts M and Allessie M A 2000 *Circulation* **102** 2650
[52] Dillon S M, Coromilas J, Waldecker B and Wit A L 1993 *J. Cardiovasc. Electrophysiol.* **4** 393
[53] Davidenko J M, Pertov A V, Salomonsz R, Baxter W and Jalife J 1992 *Nature* **355** 349
[54] Ikeda T, Yashima M, Uchida T, Hough D, Fishbein M C, Mandel W J, Chen P S and Karagueuzian H S 1997 *Circ. Res.* **81** 753
[55] Lim Z Y, Maskara B, Aguel F, Emokpae R Jr and Tung L 2006 *Circulation* **114** 2113
[56] Krinsky V I and Agladze K I 1983 *Physica* D **8** 50
[57] Steinbock O 1997 *Phys. Rev. Lett.* **78** 745
[58] Davidenko J M, Salomonsz R, Pertsov A M, Baxter W T and Jalife J 1995 *Circ. Res.* **77** 1166
[59] Bursac N and Tung L 2006 *Cardiovasc. Res.* **69** 381
[60] Agladze K, Key M W, Krinsky V and Sarvazyan N 2007 *Am. J. Physiol. Heart Circ. Physiol.* **293** 503
[61] Panfilov A V, Keldermann R H and Nash M P 2007 *Proc. Natl Acad. Sci. USA* **104** 7922
[62] Gottwald G, Purmir A and Krinsky V 2001 *Chaos* **11** 487
[63] Gaudesius G, Miragoli M, Thomas S P and Rohr S 2003 *Circ. Res.* **93** 421
[64] Miragoli M, Gaudesius G and Rohr S 2006 *Circ. Res.* **98** 801